CNRS
Centre National de la Recherche Scientifique

INFN
Instituto Nazionale di Fisica Nucleare

Constraints on the Advanced Virgo detection bench jitter from OMC alignment

L. Rolland, R. Gouaty, G. Le Corre, B. Mours, E. Tournefier

VIR-0054A-11

January 31, 2011

VIRGO * A joint CNRS-INFN Project
Project office: Traversa H di via Macerata - I-56021 S. Stefano a Macerata, Cascina (PI)
Secretariat: Telephone (39) 50 752 521 – Fax (39) 50 752 550 – e-mail virgo@pisa.infn.it

Contents

1 Introduction

In this note, we estimate limits on the jitter between the output beam of the Advanced Virgo interferometer (ITF) and the suspended detection bench. They are related to the dark fringe power variations introduced by the mis-alignment of the beam onto the output mode-cleaner (OMC).

In section 2, the ITF response is estimated in order to convert a noise that introduces dark fringe power fluctuations into its level in gravitationnal-wave strain.

The jitter between the output beam and the OMC introducess dark fringe power fluctuations through two ways

- a fraction of the incoming TEM00 power is lost,
- a fraction of the incoming high-order modes (HOM) power is seen as TEM00 mode by the OMC and is thus transmitted through.

Their contributions are calculated in section 3.

In section 4, the power variations due to the jitter are converted into equivalent strain noise and compared to the Advanced Virgo baseline design [1] sensitivity curve in order to estimate constraints on the jitter.

This study is dealing with misalignment effects. The light beam fields are thus the TEM modes (Hermite-Gaussian modes). The modes are defined in appendix A.

2 From OMC transmitted power fluctuations to equivalent gravitational strain

In this section, the response of the interferometer is described in W/m as the variations of the output power as function of the variations of the differential arm length (or the variations of the gravitional strain given a factor $L = 3000\,\mathrm{m}$).

It can then be used to estimate the strain-equivalent level of the power fluctuations due to noise, in particular the detection bench alignment jitter.

The power at the output port for a simple Michelson of contrast C depends on the power impinging on the beam-splitter[1], P_{BS}:

$$P = \frac{P_{BS}}{2}\left(1 - C\,\cos(\phi_-)\right)\frac{T_{SR}}{4} \tag{1}$$

where ϕ_- is the phase difference induced by the difference in arm lenghts, L_-. In Advanced Virgo, the TEM00 mode of the main beam (carrier) is transmitted by the signal recycling cavity with a factor $T_{SR}/4$, where T_{SR} is the transmission of the SR mirror and the factor 4 comes from the fact that the mode is not resonant in the cavity.

In an ITF with Fabry-Perot cavities of finesse $\mathcal{F}$, the average number of back and forth trips of the light in the arms is increased by $N_{arm} = 2\mathcal{F}/\pi$ (the cavities are set such that the TEM00 mode resonates). The induced phase shift is thus increased:

$$\phi_- = 2N_{arm}\frac{2\pi}{\lambda}L_- = 8\mathcal{F}\,\frac{L_-}{\lambda} \tag{2}$$

where λ is the beam wavelength.

With a DC readout [2] and around the ITF operating point $L_- = L_{off}$, the variations of differential length induce variations of output power following:

$$\frac{\mathrm{d}P}{\mathrm{d}L_-} = -\frac{CP_{BS}}{2}\,\frac{\mathrm{d}\cos(\phi_-)}{\mathrm{d}L_-}\,\frac{T_{SR}}{4} \tag{3}$$

$$= CP_{BS}\frac{2\pi N_{arm}}{\lambda}\,\sin(\phi_{off})\,\frac{T_{SR}}{4} \tag{4}$$

$$\text{where} \quad \phi_{off} = 8\mathcal{F}\,\frac{L_{off}}{\lambda} \tag{5}$$

This is the 'DC' optical response of the ITF. The arm cavities play a role above few 100 Hz which is not important for this study. In the AdV configuration, the radiation pressure plays a role below 100 Hz and the optical response vary a lot as function of the input power (see

[1] In Advanced Virgo configuration, P_{BS} includes the power recycling gain.

plot "$DARM$ to ASY_DC" on p.7 of Virgo note [3]). In the following, We define the scaling factor γ_{RP} in order to take into account these effects. For injection power lower than 25 W, the optical response (W/m) is higher than this simple computation above 10 Hz: $\gamma_{RP} > 1$. For higher power, the optical response (W/m) is lower below a few 10's of Hz: $\gamma_{RP} < 1$. Between 10 Hz and 100 Hz, this factor is in the range $[0.05; 100]$ depending on the injection power.

The nominal power at the output port is P_{00}. Let's write $\delta P(f)$ its variations around this value. The equivalent variations of differential arm length are then computed as:

$$\delta L_- = \frac{\delta P}{dP/dL_-} = \frac{1}{\gamma_{RP}} \frac{\delta P(f)}{C P_{BS}} \frac{\lambda}{2\pi N_{arm}} \frac{1}{\sin(\phi_{off})} \frac{T_{SR}}{4} \tag{6}$$

Replacing P_{BS} by its expression (from equation 1) as function of the nominal output power P_{00}:

$$\delta L_- = \frac{\delta P(f)}{P_{00}} \frac{1}{\gamma_{RP}} \frac{1 - C\cos(\phi_{off})}{2C} \frac{\lambda}{4\mathcal{F}} \frac{1}{\sin(\phi_{off})} \tag{7}$$

$$\delta h = \frac{\delta L_-}{L} \qquad \text{with } L = 3000\,\text{m} \tag{8}$$

Developping the cos and sin since $\phi_{off} \ll 1$ and neglecting[2] the term $\frac{1-C}{2C}$ in front of $\frac{\phi_{off}^2}{4}$, the equation becomes:

$$\delta L_- \sim \frac{\delta P(f)}{P_{00}} \frac{1}{\gamma_{RP}} \frac{\lambda}{4\mathcal{F}} \frac{\phi_{off}}{4} \tag{9}$$

$$\sim \frac{\delta P(f)}{P_{00}} \frac{1}{\gamma_{RP}} \frac{L_{off}}{2} \tag{10}$$

It shows that the effect is, at first order, independant on the ITF contrast C, the arm cavity finesse F and the SR mirror transmission T_{SR}, and is linear with the differential arm offset at the operating point, L_{off}.

[2] the neglected term represents 10% of the other if $1 - C = 10^{-4}$ and 1% of $1 - C = 10^{-5}$.

3 Dark fringe power variations due to misalignment

The OMC is designed in order to transmit the TEM00 mode and reflect the high-order modes (HOM). In this section, the effect of a relative mis-alignment (in translation or in rotation) between the OMC (detection bench) and the output beam is studied. When the beam is misaligned, part of the incoming TEM00 field is seen as higher-order modes in the OMC basis and is therefore not transmitted. Inversely, part of the incoming HOM fields is seen as TEM00 mode in the OMC basis and is therefore transmitted. The two effects add up in the expression of the dark fringe power transmitted by the OMC.

The Hermite-Gaussiann modes (TEMmn modes) are described in appendix A. As described in appendix C, the coupling between the modes is computed as the inner product of the misaligned HOM with the OMC TEM00 mode. Some other useful calculations are done in appendix B.

For a given translation of the incident beam wrt the OMC optical axis, one can choose the x-axis of the OMC basis to be along this translation. For a given tilt of the incident beam wrt the OMC optical axis, one can choose the y-axis of the OMC basis to be the tilt axis. Therefore, the calculations are made along a single dimension.

The beam waist is supposed to be correctly adapted to the OMC waist.

The OMC TEM00 mode is described as:

$$u_0(x) \quad = \quad \sqrt{\frac{\sqrt{2}}{\sqrt{\pi}x_0}}\, e^{-\frac{x^2}{x_0^2}} \tag{11}$$

3.1 TEM00 power losses due to OMC mis-alignment

The losses of the incident TEM00 beam due to a mis-alignment of the beam with respect to the OMC optical axis are estimated, in translation and in rotation.

3.1.1 Losses due to a translation of mode TEM00

Let's assume the incoming TEM00 beam is shifted by the distance a related to the OMC optical axis: in the OMC basis, the incoming field is defined as $u_0(x-a)$. The OMC will then see the beam as a superposition of different modes in its own TEM mode basis. The x-axis is set along the beam shift direction so that the beam amplitude depending on y is not modified. The calculation is done going up to the 2nd order in a.

The beam amplitude function is described along its propagation direction z as:

$$\phi(x,y,t,a) \quad = \quad A(t) \times u_0(x-a) \times u_0(y) \; = \; \mathcal{A}(t,y) \times u_0(x-a) \tag{12}$$

The beam amplitude that is trasmitted by the OMC is the part projected onto its TEM00 mode. This fraction is computed in appendix (see equation 88) as:

$$C^{a}_{0\to 0} = \int_{-\infty}^{-\infty} u_0^*(x-a)\, u_0(x)\, \mathrm{d}x \;\; = \;\; 1 - \frac{1}{2}\frac{a^2}{x_0^2} + \mathcal{O}(a^3) \tag{13}$$

Defining $X = \frac{a}{x_0}$ gives the transmitted beam amplitude function:

$$\phi_{00}(x,y,t,a) \;\; \sim \;\; A(t) u_0(y) \left[\left(1 - \frac{1}{2}X^2\right) u_0(x) + \mathcal{O}(X^3) \right] \tag{14}$$

Another way to estimate this fraction is given in appendix D.1.

3.1.2 Losses due to a tilt of mode TEM00

Let's assume that the incident TEM00 beam axis is tilted by the angle α with respect to the OMC axis.

The y-axis is choosen as the rotation axis of the beam: the component of the field along y is not modified. The calculation is done going up to the 2nd order in α. The beam amplitude function is described along its propagation direction z as:

$$\phi(x,y,t,\alpha) \;\; = \;\; A(t) \times u_0(x,\alpha) \times u_0(y) \; = \; \mathcal{A}(y,t) \times u_0(x,\alpha) \tag{15}$$

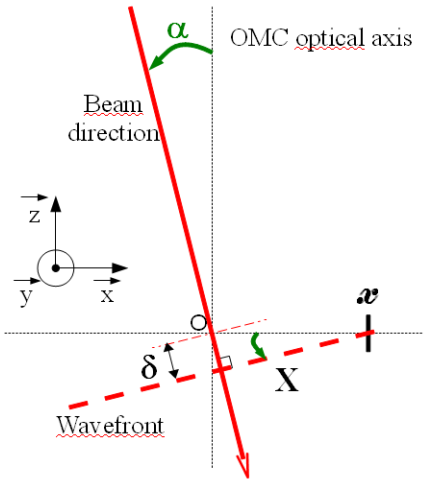

Figure 1: ***Misaligned beam wrt the OMC optical axis.*** *The OMC basis is shown on the left. The field in x takes the value of the aligned beam at the distance X of its propagation axis ; when passing in x, the field has travelled a distance δ more than the aligned beam.*

From figure 1, the beam amplitude as seen by the detector in the (x,z) area has two effects:

- the amplitude in x takes the value of the amplitude at $X = x \times \cos(\alpha) \sim x\big(1 - \frac{\alpha^2}{2} + \mathcal{O}(\alpha^4)\big)$
- the beam in x has travelled $x \times \sin(\alpha) \sim x\alpha + \mathcal{O}(\alpha^3)$ more than when there is not tilt: this induces a phase shift $\frac{2\pi x\alpha}{\lambda}$ of the beam amplitude, where λ is the laser wavelength.

The incoming beam is thus described in the OMC basis as:

$$u_0(x,\alpha) \quad = \quad u_0(x)\, e^{\frac{x^2\alpha^2}{x_0^2}}\; e^{-\frac{x^2\alpha^4}{4x_0^2}}\; e^{\mathrm{j}\frac{2\pi x\alpha + \mathcal{O}(\alpha^3)}{\lambda}} \tag{16}$$

The fraction of the beam that is trasmitted by the OMC is the part projected onto its TEM00 mode (see equation 89):

$$C^{\alpha}_{0\to 0} \quad = \quad \int_{-\infty}^{-\infty} u_0^*(x,\alpha)\, u_0(x)\, \mathrm{d}x \tag{17}$$

$$= \quad 1 + \alpha^2\big(\frac{1}{4} - \frac{1}{2\theta_D^2}\big) \qquad \text{with } \theta_D = \frac{\lambda}{\pi x_0} \tag{18}$$

$$\sim \quad 1 - \frac{\alpha^2}{2\theta_D^2} \qquad \text{since } x_0/\lambda \gg 1 \tag{19}$$

Defining $X = \frac{\alpha}{\theta_D}$ gives the transmitted beam amplitude function:

$$\phi_{00}(x,y,t,\alpha) \quad \sim \quad A(t)u_0(y)\left[\big(1 - \frac{1}{2}X^2\big)u_0(x) + \mathcal{O}(X^3)\right] \tag{20}$$

The same result is found in appendix D.2.

3.2 Leakage of the high-order TEM modes to the OMC TEM00 mode

In this section, we estimate the fraction of HOM of the incoming beam that couples to the TEM00 of the OMC and is therefore transmitted to the dark fringe photodiodes.

3.2.1 Translated incoming TEM01 to OMC TEM00

According to equation 62, the first order mode misaligned by a quantity a along the x-axis is described as:

$$u_1(x-a) \quad = \quad u_0(x-a)\, 2\frac{x-a}{x_0} \tag{21}$$

The coupling between the modes is estimated (see equation 96) as:

$$C^{a}_{1\to 0} \quad = \quad \int u_1^*(x-a)\, u_0(x)\, \mathrm{d}x \tag{22}$$

$$= \quad -\frac{a}{x_0} + \mathcal{O}(a^3) \tag{23}$$

3.2.2 Translated incoming TEM02 to OMC TEM00

According to equation 63, the second order mode misaligned by a quantity a along the x-axis is described as:

$$u_2(x-a) = u_0(x-a)\frac{1}{\sqrt{2}}\Big(\frac{4(x-a)^2}{x_0^2}-1\Big) \tag{24}$$

The coupling between the modes is estimated (see equation 100) as:

$$C_{2\to0}^{a} = \int u_2^*(x-a)\,u_0(x)\,\mathrm{d}x \tag{25}$$

$$= \frac{1}{\sqrt{2}}\frac{a^2}{x_0^2} + \mathcal{O}(a^4) \tag{26}$$

3.2.3 Tilted incoming TEM01 to OMC TEM00

According to equations 61 and 62 and to the tilted field modifications described in 3.1.2, the first order mode tilted by an angle α around the y-axis is described in the OMC basis as:

$$u_1(x,\alpha) = \sqrt{\frac{1}{\sqrt{2\pi}x_0}}\frac{2\sqrt{2}x}{x_0}\big(1-\frac{\alpha^2}{2}+\mathcal{O}(\alpha^4)\big)\,e^{-\frac{x^2}{{x_0}^2}(1-\frac{\alpha^2}{2}+\mathcal{O}(\alpha^4))^2}\,e^{\mathrm{j}\frac{2\pi x\alpha+\mathcal{O}(\alpha^3)}{\lambda}} \tag{27}$$

$$= u_0(x)\frac{2x}{x_0}\big(1-\frac{\alpha^2}{2}+\mathcal{O}(\alpha^4)\big)e^{\frac{x^2\alpha^2+\mathcal{O}(\alpha^4)}{x_0^2}}\,e^{\mathrm{j}\frac{2\pi x\alpha}{\lambda}+\mathcal{O}(\alpha^3)} \tag{28}$$

The coupling between the modes is estimated (see equation 104) as:

$$C_{1\to0}^{\alpha} = \int_{-\infty}^{+\infty} u_1^*(x,\alpha)\,u_0(x)\,\mathrm{d}x \tag{29}$$

$$= -\mathrm{j}\frac{\alpha}{\theta_D}+\mathcal{O}(\alpha^3) \tag{30}$$

3.2.4 Tilted incoming TEM02 to OMC TEM00

According to equations 61 and 63 and to the tilted field modifications described in 3.1.2, the second order mode tilted by an angle α around the y-axis is described in the OMC basis as:

$$u_2(x,\alpha) = u_0(x-\frac{x\alpha^2}{2}+\mathcal{O}(\alpha^4))\,\frac{1}{\sqrt{2}}\,\big(\frac{4}{x_0^2}(x-\frac{x\alpha^2}{2}+\mathcal{O}(\alpha^4))^2-1\big)\,e^{\mathrm{j}\frac{2\pi x\alpha+\mathcal{O}(\alpha^3)}{\lambda}} \tag{31}$$

$$= \frac{1}{\sqrt{2}}u_0(x)\,\big(1+\frac{x^2\alpha^2}{x_0^2}+\mathcal{O}(\alpha^4)\big)\big(\frac{4x^2-4x^2\alpha^2+\mathcal{O}(\alpha^4)}{x_0^2}-1\big)\big(1+\mathrm{j}\frac{2\pi x\alpha}{\lambda}-\frac{2\pi^2x^2\alpha^2}{\lambda^2}+\mathcal{O}(\alpha^3)\big) \tag{32}$$

The coupling between the modes is estimated (see equation 109) as

$$C^{\alpha}_{2\to 0} = \int_{-\infty}^{+\infty} u_2^*(x,\alpha)\, u_0(x)\, \mathrm{d}x \tag{33}$$

$$= -\frac{\alpha^2}{\sqrt{2}}\left(\frac{1}{\theta_D^2}+\frac{1}{2}\right) \qquad \text{with } \theta_D = \frac{\lambda}{\pi x_0} \tag{34}$$

$$\sim -\frac{1}{\sqrt{2}}\frac{\alpha^2}{\theta_D^2} \qquad \text{since } x_0/\lambda \gg 1 \tag{35}$$

3.3 Effect of mis-alignments on OMC output power

The effect of the misalignments in translation a and in rotation α between the output beam and the OMC on the dark fringe power is estimated.

We assume that the OMC transmits the incident TEM00 mode without losses and reflects the incident HOM. We define $P^{in}_{mn}(x,y)$ the power of the mode TEMmn at the input of the OMC.

The power at the output of the OMC can be written using the results from previous sections[3]:

$$P^{out}_{00}(x,y,a,\alpha) = |\phi_{00}(x,y)\left(1-\frac{a^2}{2x_0^2}\right)\left(1-\frac{\alpha^2}{2\theta_D^2}\right)|^2 \tag{36}$$

$$+|\phi_{01}(x,y)\left(-\frac{a}{x_0}-\mathrm{j}\frac{\alpha}{\theta_D}\right)|^2 \tag{37}$$

$$+|\phi_{02}(x,y)\frac{1}{\sqrt{2}}\left(\frac{a^2}{x_0^2}-\frac{\alpha^2}{\theta_D^2}\right)|^2 \tag{38}$$

$$= P^{in}_{00}\left(1-\frac{a^2}{x_0^2}-\frac{\alpha^2}{\theta_D^2}\right) \tag{39}$$

$$+P^{in}_{10}\left(\frac{a^2}{x_0^2}+\frac{\alpha^2}{\theta_D^2}\right) \tag{40}$$

$$+P^{in}_{20}\left(\frac{a^4}{2x_0^4}+\frac{\alpha^4}{2\theta_D^4}-\frac{a^2\alpha^2}{x_0^2\theta_D^2}\right) \tag{41}$$

keeping only the lowest order terms in a, $alpha$ and α for each component.

[3] The leakages from the translated 3rd order mode field has been also calculted: $P^{out}_{00}(x,y,a) = P^{in}_{30}(-\frac{1}{\sqrt{6}}\frac{a^3}{x_0^3}) + \mathcal{O}(a^5)$.

4 Constraints on the jitter between the output beam and the detection bench

The variations of OMC output power related to TEM00 losses and high-order modes leakages have been estimated in equation 39. We have defined a parameter X used to described the jitter in translation: $X_a = \frac{a}{x_0}$ and in rotation: $X_\alpha = \frac{\alpha}{\theta_D}$.

4.1 Constraints on the jitter RMS

Choosing the power losses or leakage to be less than $\epsilon = 1\%$ of the nominal power transmitted by the OMC, one can set constraints on the value of X. This value can be used as an estimation of X^{rms}.

4.1.1 Constraints from TEM00 losses

Choosing the loose less than ϵ of the incident TEM00 power due to the X offset, the maximum acceptable value of X is $X_{00}^{rms} = \sqrt{\epsilon} = 0.1$. The corresponding constraints on the translation and rotation are given in the table 3.

4.1.2 Constraints from first order mode power leakages

The TEMmn modes with $m+n = 1$ that are incident onto the OMC are related with misalignments of the ITF. A preliminary estimation of their power in Advanced Virgo is done scaling the powers measured in Virgo+ by the ITF input power.

In October 2010[4], the OMC length has been scanned (during ∼15 minutes) and the transmitted beam has been imaged in order to determine the resonating modes. In parallel, the power of the modes have been measured, as shown figure 2. The powers in the modes TEM10, TEM01 have been estimated to ∼ 135 mW each. The power of the ITF input beam (after input mode-cleaner) was 17 W.

Assuming the HOM powers scale with the ITF input power, a factor $\frac{125}{17}$ can be applied, yielding to powers of ∼1 W for the modes TEM01 and TEM10. In principle, the powers in Advanced Virgo are expected to be lower since the Advanced Virgo will have *stable* recycling cavities wrt to Virgo with *marginally stable cavities*: the HOM should be better suppressed in Advanced Virgo.

In Advanced Virgo, the expected power on the TEM00 mode [4] is of the order of $P_{00} =$ 70 mW.

From equation 39, the fraction of first order mode power that leaks onto the TEM00 mode of the mis-aligned OMC is $P_{10}^{in} \times X^2$. Choosing that the contribution from the high-order modes

[4] See logbook entry 28251.

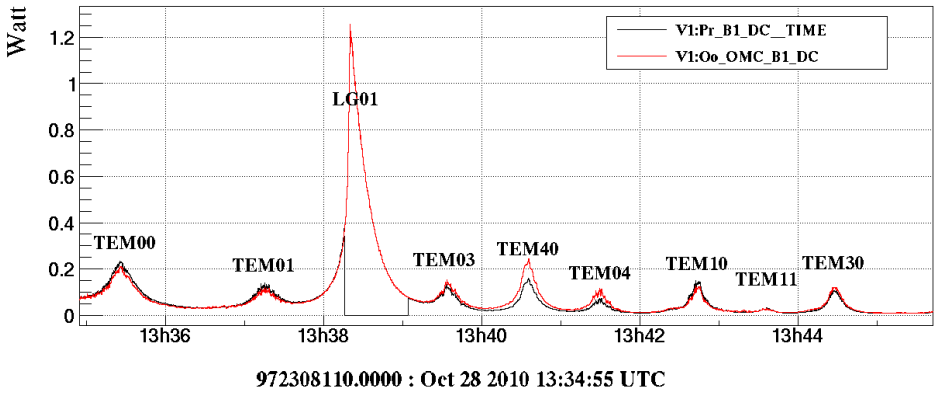

Figure 2: ***Power of the modes incident on the OMC in Virgo+ (October 2010).*** *For each resonance, the beam has been imaged in order to determine the transmitted mode that is labeled. TEM: Hermite-Gauss modes. LG: Laguerre-Gauss modes.*

to the OMC transmitted power is less than ϵ, the maximum acceptable value of X^2 is $\epsilon \times \frac{P_{00}}{P_{10}}$. For an input power of 125 W, it yields[5] $X_{01}^{rms} < X_{00}^{rms}\sqrt{\frac{P_{00}}{P_{10}}} = 0.1 \times \sqrt{0.07/1} = 0.026$.

The constraints from the leakage of the first order modes to the fundamental mode of the OMC are thus a factor 4 stronger than the one coming from the losses of the incident fundamental mode described section 4.1.

4.1.3 Constraints from the second order mode power leakages

The TEMmm modes ($m+n=2$) are related to the first Laguerre-Gauss mode (LG01, LG10). In Advanced Virgo, the power in the Laguerre-Gauss HOM is expected to be of the order of four time the power in the fundamental mode [4].

Assuming $P_{20}^{in} \sim 4P_{00}^{in}$ and choosing that the leakage of these modes represent less than ϵ of the OMC transmitted beam, the maximum acceptable value of X^4 is $2\epsilon\frac{P_{00}^{in}}{P_{20}^{in}}$. For an input power of 125 W, it yields $X_{02}^{rms} < \sqrt{X_{00}^{rms}} \times \left(2\frac{P_{00}^{in}}{P_{20}^{in}}\right)^{1/4} = 0.26$.

Scaling the power of the LG01 mode measured in Virgo+ with monolithic suspension yields to larger constraints: $X < 0.1$, which is of the same order of magnitude. However, the LG01 mode in Virgo+ is large due to the mismatch between the waists of the beam in the two Fabry-Perot cavities. It is thus expected that this constraint is too strong.

[5] We keep two independent analysis of the TEM00 losses with quite robust hypothesis, and the HOM leakages with much more uncertainties on the assumed HOM powers.

4.1.4 Specification on the jitter RMS

The maximum acceptable of the jitter in translation or rotation, given as X and related to the different modes of the incident beam are summarized in table 1.

	TEM00 losses	TEMmn $(m+n=1)$ leakages	TEMmn $(m+n=2)$ leakages
X^{rms}	0.1	0.026	0.26

Table 1: Maximum value of X estimated in order to have less than 1% of losses of the TEM00 mode and less than 1% leakage of the HOM into the TEM00 mode (in the case of an input power of 125 W). These values can be used as estimations of X^{rms}.

The stronger constraints is coming from the leakage of the 1st TEM modes onto the OMC TEM00 mode. Due to the way the power of the 1st order modes have been extrapolated from Virgo+ to Advanced Virgo, this contraint might be too tight but it is used in the following to estimate the constraint on the relative jitter between the beam and the detection bench.

4.2 Frequency-dependent constraints on the jitter

The constraints on the RMS of the relative alignment between the OMC and the incoming beam can be extended to estimate constraints as function of frequency. The way this extension is applied is first explained and is then used to derive constraints.

4.2.1 From jitter RMS to frequency-dependent specifications

From the Advanced Virgo design sensitivity and equations 7 and 39, it is possible to define constraints on the relative jitter (in translation and rotation) between the OMC and the ITF output beam.

One wants the strain equivalent noise $\delta L_-^{(OMC)}$ from this jitter to be below the design sensitivity δL_-^{design} with a margin factor γ. From equation 39, the power variations δP due to a jitter on X can be written as:

$$\frac{\delta P(f)}{P_{00}(f)} = X^2 \quad \text{for the TEM00 losses} \tag{42}$$

$$\frac{\delta P(f)}{P_{00}(f)} = \frac{P_{10}}{P_{00}} X^2 \quad \text{for the 1st HOM leakages} \tag{43}$$

$$\frac{\delta P(f)}{P_{00}(f)} = \frac{P_{20}}{P_{00}} \frac{X^4}{2} \quad \text{for the 2nd HOM leakages} \tag{44}$$

These power variations are reported in equation 7 in order to estimate their effect on the Advanced Virgo sensitivity.

The noise introduced by $\frac{\delta P(f)}{P_{00}(f)}$, can be written as:

$$\delta L_-^{(X)} = \frac{\delta P(f)}{P_{00}(f)} \frac{1}{\gamma_{RP}} \frac{\lambda}{8\mathcal{F}} \frac{1 - C\cos(\phi_{off})}{C\sin(\phi_{off})} \tag{45}$$

The condition $\delta L_-^X < \delta L_-^{design}/\gamma$ is equivalent to:

$$\frac{\delta P(f)}{P_{00}(f)} < \frac{\delta L_-^{design}}{\gamma} \gamma_{RP} \frac{8\mathcal{F}}{\lambda} \frac{C\sin(\phi_{off})}{1 - C\cos(\phi_{off})} \tag{46}$$

$\mathcal{F}$	L_{off} (m)	$1-C$	λ (m)	OMC waist (m)	SDB waist (m)
446 [6]	10^{-11} [7]	10^{-4}	1064×10^{-9}	236×10^{-6} [8]	350×10^{-6} [4]

Table 2: Summary of used Advanced Virgo parameters.

Using the Advanced Virgo design values given in table 2, the constraint is estimated to:

$$\frac{\delta P(f)}{P_{00}(f)} < 1.7 \times 10^{11} \gamma_{RP} \frac{\delta L_-^{design}(f)}{\gamma} \tag{47}$$

$$< 5.1 \times 10^{14} \gamma_{RP} \frac{\delta h^{design}(f)}{\gamma} \tag{48}$$

Losses of the TEM00 mode - Using the power variations from the TEM00 mode (equation 42), this equation gives the constraint on the normalized variable $X^2(f)$ as function of the ITF design sensitivity $h^{design}(f)$. The parameter we want to constrain is $X(f)$.

The amplitude spectrum density $X(f)$ is expected to be dominated by the low frequency (below a few hertz). As shown in appendix A of [5], the amplitude spectrum density of X^2 can be approximated by:

$$X^2(f) \sim 2 \times X^{rms} \times X(f) \tag{49}$$

where X^{rms} is the RMS of the $X(t)$ signal.

The constraint on $X(f)$ (equation 48) coming from the TEM00 losses can be written as:

$$X_{00}^{max}(f) = 5.1 \times 10^{14} \gamma_{RP} \frac{\delta h^{design}(f)}{\gamma} \frac{1}{2X_{00}^{rms}} \tag{50}$$

The value of X_{00}^{rms} has been estimated in section 4.1.

Leakgage of the TEM01 mode - Combining equations 42 and 48, the constraints on $X^2(f)$ can be estimated. The constraint on $X(f)$ is then derived as:

$$X_{01}^{max}(f) = \frac{P_{00}}{P_{10}} 5.1 \times 10^{14} \gamma_{RP} \frac{\delta h^{design}(f)}{\gamma} \frac{1}{2X_{01}^{rms}} \quad (51)$$

$$X_{01}^{max}(f) = \sqrt{\frac{P_{00}}{P_{10}}} X_{00}^{max}(f) \quad (52)$$

The constraints on $X(f)$ from the TEM01 leakage are thus stronger than the constraints from the TEM00 losses if the ITF output power of the 1st HOM is stronger than the power of the fundamental mode.

From the estimation of the TEM01 power given above, the constraints are thus stronger by a factor ~ 4 than the one from the TEM00 losses.

Leakgage of the TEM02 mode - The power in the TEM02 mode is expected to be less than 1 W (see [4]) and its leakages are of the 4th order in jitter X. Its effect on the power transmitted by the OMC is thus negligible compared to the TEM00 losses of TEM01 leakages.

4.2.2 Estimation of the beam specifications at the level of the OMC

From previous section, the higher constraints come from the leakage of the TEM01 mode into the TEM00 mode. From its RMS value X_{01}^{rms} and equation 51 one can derive the maximum amplitude spectrum of $X(f)$.

The Advanced Virgo reference sensitivity curve from the baseline design [1] (figure 2, p.11) has been used. The values at 10 Hz, 20 Hz and 100 Hz to derive the first constraint on $X(f)$ are given in tables 3 and 4.

To estimate the constraints on a and α, the waist of the beam at the OMC has to be known. The value of the OMC beam waist is given in table 2. It implies $\theta_D = 1.4\,\mathrm{mrad}$.

The constraints have been derived for different input powers (different values of the factor γ_{PR}). They are summarized in the tables.

Concerning the estimation of the factor γ_{RP} above 10 Hz, a value of 1 has been used for $P_{in} < 25\,\mathrm{W}$. It has been approximated by $\gamma_{RP} = 10^{-3} \times f^{2.3}$ for $P_{in} = 50\,\mathrm{W}$ and $\gamma_{RP} = 10^{-4} \times f^{2.7}$ for $P_{in} = 125\,\mathrm{W}$, using 1 as maximum value.

4.3 Estimation of the beam specifications at the level of the suspended detection bench

The constraint on the beam jitter a and beam angular stability α at the level of the OMC waist can be translated into constraints at the input of the suspended detection bench. The scaling

factor is estimated from the beam waists given in table 2.

$$a_{max}^{SDB} \sim a_{max}^{OMC} \times \frac{x_{SDB}}{x_{OMC}} \quad (53)$$

$$\alpha_{max}^{SDB} \sim \alpha_{max}^{OMC} \times \frac{x_{OMC}}{x_{SDB}} \quad (54)$$

The estimated constraints are reported in table 3 and 4.

5 Summary

The dark fringe power variations introduced by mis-alignment of the ITF beam with respect to the suspended detection bench and the OMC have been estimated and converted into equivalent strain noise. Jitter specifications were extracted from the comparison of this level with the Advanced Virgo baseline sensitivity curve.

The **looser estimated constraints** that need to be fulfilled are summarized in table 3 and in figure 3. They are estimated from the TEM00 losses.
Some **tighter conservative constraints** are given in table 4 and in figure 4 They are estimated from the TEM01 leakages (assuming 1 W in the first order TEM modes).

Note that these constraints depend on the waist of the ITF output beam. For a larger beam waist, the translation constraints will be looser while the rotation constraints will be tighter.

The specifications apply both to the jitter of the Advanced Virgo detection bench and to alignment issues through the jitter of the ITF output beam.

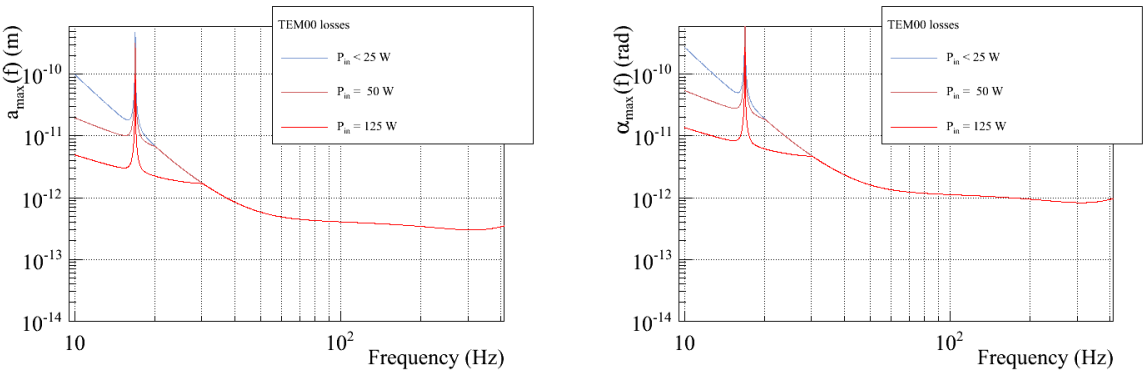

(a) Translation (b) Rotation

Figure 3: ***Jitter constraints derived from TEM00 mode losses*** *estimated for different input ITF powers.*

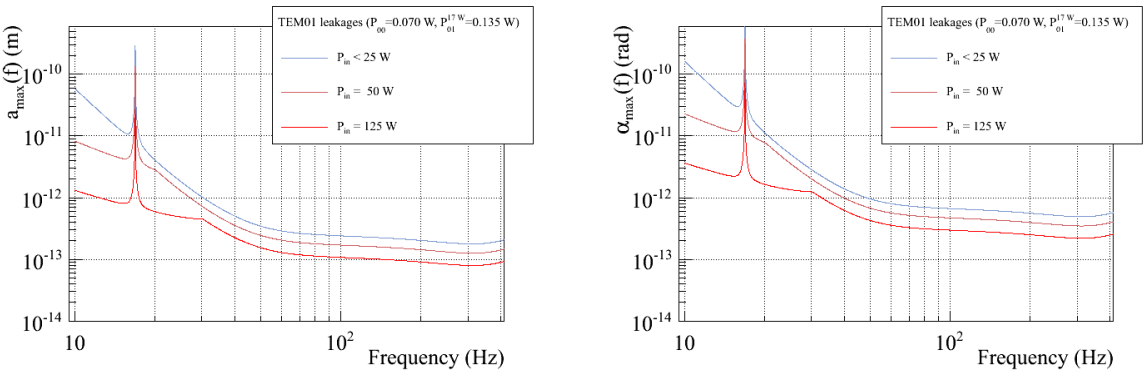

(a) Translation (b) Rotation

Figure 4: ***Jitter (conservative) constraints derived from TEM01 mode leakages*** *estimated for different input ITF powers.*

	RMS	10 Hz	20 Hz	100 Hz
δh^{design}	-	1.1×10^{-21}	7.7×10^{-23}	4.5×10^{-24}

$P < 25$ W	γ_{RP}		-	1	1	1
	OMC input	$X_{max}(f)$	0.1	2.8×10^{-7}	2.0×10^{-8}	1.2×10^{-9}
		$a_{max}(f)$ (m)	24×10^{-6}	6.6×10^{-11}	4.6×10^{-12}	2.7×10^{-13}
		$\alpha_{max}(f)$ (rad)	144×10^{-6}	4.0×10^{-10}	2.8×10^{-11}	1.7×10^{-12}
	SDB input	$a_{max}(f)$ (m)	35×10^{-6}	9.9×10^{-11}	6.9×10^{-12}	4.0×10^{-13}
		$\alpha_{max}(f)$ (rad)	97×10^{-6}	2.7×10^{-10}	1.9×10^{-11}	1.1×10^{-12}

$P = 50$ W	γ_{RP}		-	0.2	1	1
	OMC input	$X_{max}(f)$	0.1	5.6×10^{-8}	1.9×10^{-8}	1.2×10^{-9}
		$a_{max}(f)$ (m)	24×10^{-6}	1.3×10^{-11}	4.5×10^{-12}	2.7×10^{-13}
		$\alpha_{max}(f)$ (rad)	143×10^{-6}	8.1×10^{-11}	2.8×10^{-11}	1.7×10^{-12}
	SDB input	$a_{max}(f)$ (m)	35×10^{-6}	2.0×10^{-11}	6.7×10^{-12}	4.0×10^{-13}
		$\alpha_{max}(f)$ (rad)	97×10^{-6}	5.4×10^{-11}	1.9×10^{-12}	1.1×10^{-12}

$P = 125$ W	γ_{RP}		-	0.05	0.3	1
	OMC input	$X_{max}(f)$	0.1	1.4×10^{-8}	6.4×10^{-9}	1.2×10^{-9}
		$a_{max}(f)$ (m)	24×10^{-6}	3.3×10^{-12}	1.5×10^{-12}	2.7×10^{-13}
		$\alpha_{max}(f)$ (rad)	143×10^{-6}	2.0×10^{-11}	9.2×10^{-12}	1.7×10^{-12}
	SDB input	$a_{max}(f)$ (m)	35×10^{-6}	4.9×10^{-12}	2.2×10^{-12}	4.0×10^{-13}
		$\alpha_{max}(f)$ (rad)	97×10^{-6}	1.4×10^{-11}	6.2×10^{-12}	1.1×10^{-12}

Table 3: **(Minimal)constraints from the TEM00 losses.** *RMS in given units, assuming the losses represent less than 1% of the power in the TEM00 mode. Maximum values at 10 Hz, 20 Hz and 100 Hz are given in units/$\sqrt{Hz}$, with a margin factor $\gamma = 10$. Different values of γ_{RP} have been used depending on the input power P (derived from [3], p.7).*

	RMS	10 Hz	20 Hz	100 Hz
δh^{design}	-	1.1×10^{-21}	7.7×10^{-23}	4.5×10^{-24}

$P < 25$ W	γ_{RP}		-	1	1	1
	OMC input	$X_{max}(f)$	0.06	1.7×10^{-7}	1.2×10^{-8}	6.9×10^{-10}
		$a_{max}(f)$ (m)	14×10^{-6}	3.9×10^{-11}	2.7×10^{-12}	1.6×10^{-13}
		$\alpha_{max}(f)$ (rad)	85×10^{-6}	2.4×10^{-10}	1.7×10^{-11}	9.9×10^{-13}
	SDB input	$a_{max}(f)$ (m)	21×10^{-6}	5.9×10^{-11}	4.0×10^{-12}	2.4×10^{-13}
		$\alpha_{max}(f)$ (rad)	57×10^{-6}	1.6×10^{-10}	1.1×10^{-11}	6.6×10^{-13}

$P = 50$ W	γ_{RP}		-	0.2	1	1
	OMC input	$X_{max}(f)$	0.04	2.4×10^{-8}	8.0×10^{-9}	4.9×10^{-10}
		$a_{max}(f)$ (m)	9.9×10^{-6}	5.6×10^{-12}	1.9×10^{-12}	1.1×10^{-13}
		$\alpha_{max}(f)$ (rad)	60×10^{-6}	3.4×10^{-11}	1.2×10^{-11}	7.0×10^{-13}
	SDB input	$a_{max}(f)$ (m)	15×10^{-6}	8.3×10^{-12}	2.8×10^{-12}	1.7×10^{-13}
		$\alpha_{max}(f)$ (rad)	40×10^{-6}	2.2×10^{-11}	7.8×10^{-12}	4.7×10^{-13}

$P = 125$ W	γ_{RP}		-	0.05	0.3	1
	OMC input	$X_{max}(f)$	0.027	3.7×10^{-9}	1.7×10^{-9}	3.0×10^{-10}
		$a_{max}(f)$ (m)	6.3×10^{-6}	8.8×10^{-13}	4.0×10^{-13}	7.2×10^{-14}
		$\alpha_{max}(f)$ (rad)	38×10^{-6}	5.4×10^{-12}	2.4×10^{-12}	4.4×10^{-13}
	SDB input	$a_{max}(f)$ (m)	9.3×10^{-6}	1.3×10^{-12}	5.9×10^{-13}	1.1×10^{-13}
		$\alpha_{max}(f)$ (rad)	26×10^{-6}	3.6×10^{-12}	1.6×10^{-12}	3.0×10^{-13}

Table 4: **(Conservative) constraints from the TEM01 mode leakages**, *assuming* $P_{00} = 0.07$ *W and* $P_{01} = 1$ *W. RMS in given units, assuming the leakages represent less than 1% of the power in the TEM00 mode. Maximum values at 10 Hz, 20 Hz and 100 Hz are given in units/*$\sqrt{Hz}$*, with a margin factor* $\gamma = 10$*. Different values of* γ_{RP} *have been used depending on the input power P (derived from [3], p.7).*

References

[1] The Virgo collaboration, Virgo note VIR-027A-09 (2009) *Advanced Virgo Baseline Design.*

[2] E. Tournefier, Virgo note VIR-NOT-LAP-1390-338 (2007) *Technical noises for Virgo+: DC and AC readout*

[3] G. Vajente, Virgo note VIR-069A-08 (2008) *Advanced Virgo Length Sensing and control: Double demodulation vs Single demodulation.*

[4] R. Gouaty, E. Tournefier, Virgo note in prep. (2010) *Advanced Virgo output mode cleaner: revision of the specifications*

[5] R. Gouaty, PhD thesis LAPP-T-2006-02 (2006) *Analyse de la sensibilité du détecteur d'ondes graviationnalles Virgo*

[6] R.L. Ward, Virgo note VIR-0541A-10 (2010) *Advanced Virgo Optical Design Parameters Summary.*

[7] E. Tournefier, Virgo note VIR-NOT-071A-08 (2008) *Advanced Virgo output mode cleaner: specifications.*

[8] R. Gouaty, B. Mours, E. Tournefier, Virgo presentation VIR-0373A-10 (2010) *Specifications for OMC telescope in AdVirgo.*

[9] Siegman A. E., *Lasers*, University Science Books, Mill Valley, California (1986) (ISBN 0-935702-11-5)

[10] H. Kogelnik and T. Li **Applied Optics 5**, 10 (1966), *Laser Beams and Resonators*

A Definition of Hermite-Gaussian modes

The profile of a laser beam propagating along the direction z with amplitude A can be projected on the base of the Hermite-Gaussian modes $u_n(x,z)$:

$$\Phi_{n,m}(x,y,z) = A(t) \times u_n(x,z) \times u_m(y,z) \tag{55}$$

The waists of the beam, called x_0 and y_0, can be different along the two axis. In the following, since the description along the two axis can be separated, we only consider one dimension, x.

We consider a beam propagating along the z-axis with the waist position at $z = 0$. In the following, the calculus are made at $z = 0$.

From Siegman [9] (p. 686) the nth Hermite-Gaussian mode amplitude functions **at the waist position**[6] can be written:

$$u_n(x, z=0) = \left(\frac{2}{\pi}\right)^{1/4} \left(\frac{1}{2^n n!\, x_0}\right)^{1/2} \times H_n\left(\frac{\sqrt{2}x}{x_0}\right) \times e^{-\frac{x^2}{x_0^2}} \tag{56}$$

where H_n are the unnormalized Hermite polynomials. The first few polynomials are given by:

$$H_0(v) = 1 \qquad H_1(v) = 2v \tag{57}$$
$$H_2(v) = 4v^2 - 2 \qquad H_3(v) = 8v^3 - 12v \tag{58}$$
$$H_4(v) = 16v^4 - 48v^2 + 12 \qquad H_5(v) = 32v^5 - 160v^3 + 120v \tag{59}$$

In fact, the beam profile of amplitude A has two dimensions:

$$\Phi_{n,m}(x,y,z=0) = A(t) \times u_n(x,z=0) \times u_m(y,z=0) \tag{60}$$

The waists x_0 and y_0 can be different. In this note, we assume they are equals.

We can derive the first Hermite-Gaussian mode amplitude functions as function of the first order mode:

$$u_0(x,z=0) = \left(\frac{\sqrt{2}}{\sqrt{\pi}x_0}\right)^{1/2} e^{-\frac{x^2}{x_0^2}} = u_0(x) \tag{61}$$

$$u_1(x,z=0) = \left(\frac{1}{\sqrt{2\pi}x_0}\right)^{1/2} \frac{2\sqrt{2}x}{x_0}\, e^{-\frac{x^2}{x_0^2}} = u_0(x)\frac{2x}{x_0} \tag{62}$$

$$u_2(x,z=0) = \left(\frac{1}{4\sqrt{2\pi}x_0}\right)^{1/2} \left(\frac{8x^2}{x_0^2} - 2\right) e^{-\frac{x^2}{x_0^2}} = u_0(x)\frac{1}{\sqrt{2}}\left(\frac{4x^2}{x_0^2} - 1\right) \tag{63}$$

[6] Being at the waist position, $z = 0$, we assume that, in equation 28 from [10], the Gouy phase is null ($\Phi = 0$), the beam radius is the waist $\omega = \omega_0$ and the radius of curvature of the wavefront is null $R = 0$.

B Some integral calculations

The following terms are found in the process of computing such coupling factors. Their computation is detailed here.

$$\int_{-\infty}^{+\infty} e^{-\beta x^2}\,\mathrm{d}x = \sqrt{\frac{\pi}{\beta}} \tag{64}$$

$$\int_{-\infty}^{+\infty} u_0^*(x)\,x^n\,u_0(x)\,\mathrm{d}x = \int x^n\,e^{-\frac{2x^2}{x_0^2}}\,\mathrm{d}x = 0 \quad \text{if } n \text{ is an odd number (odd function)} \tag{65}$$

$$\int_{-\infty}^{+\infty} u_0^*(x)\,x^2\,u_0(x)\,\mathrm{d}x = \frac{\sqrt{2}}{\sqrt{\pi}x_0}\int x^2\,e^{-\frac{2x^2}{x_0^2}}\,\mathrm{d}x \tag{66}$$

$$= \frac{\sqrt{2}}{\sqrt{\pi}x_0}\frac{x_0^2}{2\sqrt{2}}\frac{\sqrt{\pi}x_0}{2} \tag{67}$$

$$= \frac{x_0^2}{4} \quad \text{(integrating by parts)} \tag{68}$$

$$\int_{-\infty}^{+\infty} u_0^*(x)\,x^4\,u_0(x)\,\mathrm{d}x = \frac{\sqrt{2}}{\sqrt{\pi}x_0}\int x^4\,e^{-\frac{2x^2}{x_0^2}}\,\mathrm{d}x \tag{69}$$

$$= \frac{3}{16}x_0^4 \quad \text{(integrating by parts)} \tag{70}$$

$$\int_{-\infty}^{+\infty} u_0^*(x)\,x^6\,u_0(x)\,\mathrm{d}x = \frac{15}{64}x_0^6 \tag{71}$$

$$\int_{-\infty}^{+\infty} u_0^*(x)\,x^8\,u_0(x)\,\mathrm{d}x = \frac{105}{256}x_0^8 \tag{72}$$

$$\int_{-\infty}^{-\infty} u_0^*(x-a)\,x\,u_0(x)\,\mathrm{d}x = \frac{\sqrt{2}}{\sqrt{\pi}x_0}\int e^{-\frac{(x-a)^2}{x_0^2}}\,x\,e^{-\frac{x^2}{x_0^2}}\mathrm{d}x \tag{73}$$

$$= \int u_0^*(x)\,x\,u_0(x)\big(1-\frac{a^2}{x_0^2}+\frac{2ax}{x_0^2}+\frac{2a^2x^2}{x_0^4}+\mathcal{O}(a^3)\big)\mathrm{d}x \tag{74}$$

$$= \frac{2ax}{x_0^2}\frac{x_0^2}{4}+\mathcal{O}(a^3) \tag{75}$$

$$= \frac{a}{2}+\mathcal{O}(a^3) \tag{76}$$

$$\int_{-\infty}^{-\infty} u_0^*(x-a)\,x^2\,u_0(x)\,\mathrm{d}x = \frac{\sqrt{2}}{\sqrt{\pi}x_0}\int e^{-\frac{(x-a)^2}{x_0^2}}\,x^2\,e^{-\frac{x^2}{x_0^2}}\mathrm{d}x \quad (77)$$

$$= \int u_0^*(x)\,x^2\,u_0(x)\big(1-\frac{a^2}{x_0^2}+\frac{2ax}{x_0^2}+\frac{2a^2x^2}{x_0^4}+\mathcal{O}(a^3)\big)\mathrm{d}x \quad (78)$$

$$= \big(1-\frac{a^2}{x_0^2}\big)\frac{x^2}{4}+\big(\frac{2a^2}{x_0^4}\big)\big(\frac{3x_0^4}{16}\big)+\mathcal{O}(a^3) \quad (79)$$

$$= \frac{x_0^2}{4}+\frac{a^2}{8}+\mathcal{O}(a^3) \quad (80)$$

C Coupling between TEM modes

The TEM modes in the OMC form a basis where the incoming beam can be projected. An incoming light field u^{in} can have a component along the mode $u_0(x)$ of the OMC that will be transmitted by the OMC. It can be computed as the inner product of the fields: the coupling between the u^{in} and u_0 is written as:

$$C_{in\to 0} = \int_{-\infty}^{+\infty} u_{in}^*(x)\,u_0(x)\,\mathrm{d}x \quad (81)$$

where * stands for the complex conjugate. The TEM fields are normalized such that

$$C_{0\to 0} = \int_{-\infty}^{+\infty} u_0^*(x)\,u_0(x)\,\mathrm{d}x = 1 \quad (82)$$

C.1 Calculations for TEM00 power losses

$$\int_{-\infty}^{-\infty} u_0^*(x-a)\,u_0(x)\,\mathrm{d}x = \frac{\sqrt{2}}{\sqrt{\pi}x_0}\int e^{-\frac{(x-a)^2}{x_0^2}}\,e^{-\frac{x^2}{x_0^2}}\,\mathrm{d}x \quad (83)$$

$$= \frac{\sqrt{2}}{\sqrt{\pi}x_0}\int e^{-\frac{x^2}{x_0^2}}\,e^{-\frac{a^2}{x_0^2}}e^{\frac{2ax}{x_0^2}}\,e^{-\frac{x^2}{x_0^2}}\,\mathrm{d}x \quad (84)$$

$$= \frac{\sqrt{2}}{\sqrt{\pi}x_0}\int e^{-2\frac{x^2}{x_0^2}}\,\big(1-\frac{a^2}{x_0^2}+\mathcal{O}(a^4)\big)\big(1+\frac{2ax}{x_0^2}+\frac{2a^2x^2}{x_0^4}+\mathcal{O}(a^3)\big)\mathrm{d}x \quad (85)$$

$$= \int u_0^*(x)\,u_0(x)\big(1-\frac{a^2}{x_0^2}+\frac{2ax}{x_0^2}+\frac{2a^2x^2}{x_0^4}+\mathcal{O}(a^3)\big)\mathrm{d}x \quad (86)$$

$$= 1-\frac{a^2}{x_0^2}+\frac{2a^2}{x_0^4}\frac{x_0^2}{4}+\mathcal{O}(a^3) \quad (87)$$

$$= 1-\frac{1}{2}\frac{a^2}{x_0^2}+\mathcal{O}(a^3) \quad (88)$$

$$C^{\alpha}_{0\to 0} = \int_{-\infty}^{-\infty} u_0^*(x,\alpha)\, u_0(x)\, \mathrm{d}x \tag{89}$$

$$= \frac{\sqrt{2}}{\sqrt{\pi}x_0} \int e^{\frac{-8+4\alpha^2+\mathcal{O}(\alpha^4)}{4x_0^2}x^2}\, e^{-\mathrm{j}\frac{2\pi\alpha+\mathcal{O}(\alpha^3)}{\lambda}x}\, \mathrm{d}x \tag{90}$$

$$= \int u_0^*(x)u_0(x)\big(1+\frac{x^2\alpha^2}{x_0^2}+\mathcal{O}(\alpha^4)\big)\big(1+\mathcal{O}(\alpha^4)\big)\big(1-j\frac{2\pi x\alpha}{\lambda}-2\big(\frac{\pi x\alpha}{\lambda}\big)^2+\mathcal{O}(\alpha^3)\big)\mathrm{d}x \tag{91}$$

$$= \int u_0^*(x)u_0(x)\big(1-\mathrm{j}\frac{2\pi\alpha}{\lambda}x+(\frac{\alpha^2}{x_0^2}-2\frac{\pi^2\alpha^2}{\lambda^2})x^2+\mathcal{O}(\alpha^3)\big)\mathrm{d}x \tag{92}$$

$$= 1-0+\big(\frac{\alpha^2}{x_0^2}-2\frac{\pi^2\alpha^2}{\lambda^2}\big)\frac{x_0^4}{4} \tag{93}$$

$$= 1+\alpha^2\big(\frac{1}{4}-\frac{1}{2\theta_D^2}\big) \qquad \text{with } \theta_D=\frac{\lambda}{\pi x_0} \tag{94}$$

$$\sim 1-\frac{\alpha^2}{2\theta_D^2} \qquad \text{since } x_0/\lambda \gg 1 \tag{95}$$

C.2 Calculations for high-order mode leakages

Using equations 88 and 76:

$$C^{a}_{1\to 0} = \int u_1^*(x-a)\, u_0(x)\, \mathrm{d}x \quad = \quad \int u_0^*(x-a)\, \frac{2(x-a)}{x_0}\, u_0(x)\mathrm{d}x \tag{96}$$

$$= -\frac{2a}{x_0}\int u_0^*(x-a)\, u_0(x)\mathrm{d}x \;+\; \frac{2}{x_0}\int u_0^*(x-a)\, x\, u_0(x)\mathrm{d}x \tag{97}$$

$$= -\frac{2a}{x_0}\big(1-\frac{a^2}{2x_0^2}+\mathcal{O}(a^4)\big) \;+\; \frac{2}{x_0}\frac{a}{2}\big(1-\frac{a^2}{2x_0^2}+\mathcal{O}(a^4)\big) \tag{98}$$

$$= -\frac{a}{x_0} \;+\; \mathcal{O}(a^3) \tag{99}$$

Using equations 88, 76 and 80:

$$C^{a}_{2\to 0} = \int u_2^*(x-a)\, u_0(x)\, \mathrm{d}x \tag{100}$$

$$= \frac{1}{\sqrt{2}}\big(\frac{4a^2}{x_0^2}-1\big)\int u_0^*(x-a)\, u_0(x)\, \mathrm{d}x \quad + \quad \frac{1}{\sqrt{2}}\frac{-8a}{x_0^2}\int u_0^*(x-a)\, x\, u_0(x)\, \mathrm{d}x \tag{101}$$

$$+ \quad \frac{1}{\sqrt{2}}\frac{4}{x_0^2}\int u_0^*(x-a)\, x^2\, u_0(x)\, \mathrm{d}x \tag{102}$$

$$= \frac{1}{\sqrt{2}}\frac{a^2}{x_0^2} \;+\; \mathcal{O}(a^4) \tag{103}$$

Using equations 88 and 76:

$$C^{\alpha}_{1\to 0} = \int_{-\infty}^{+\infty} u_1^*(x,\alpha)\, u_0(x)\,\mathrm{d}x \tag{104}$$

$$= \int u_0^*(x)\frac{2x}{x_0}u_0(x)\left(1-\frac{\alpha^2}{2}+\mathcal{O}(\alpha^4)\right)\left(1+\frac{x^2\alpha^2}{x_0^2}+\mathcal{O}(\alpha^4)\right)\left(1-\mathrm{j}\frac{2\pi x\alpha}{\lambda}-\frac{4\pi^2x^2\alpha^2}{\lambda^2}+\mathcal{O}(\alpha^3)\right)\mathrm{d}x \tag{105}$$

$$= \frac{2}{x_0}\int u_0^*(x)xu_0(x)\left(1-\mathrm{j}\frac{2\pi\alpha}{\lambda}x+\alpha^2(-\frac{1}{2}+\frac{x^2}{x_0^2}-\frac{4\pi^2x^2}{\lambda^2})+\mathcal{O}(\alpha^3)\right)\mathrm{d}x \tag{106}$$

$$= -\mathrm{j}\frac{4\pi\alpha}{x_0\lambda}\frac{x_0^2}{4}+\mathcal{O}(\alpha^3) \tag{107}$$

$$= -\mathrm{j}\frac{\alpha}{\theta_D}+\mathcal{O}(\alpha^3) \tag{108}$$

Using equations 82, 65, 68 and 70:

$$C^{\alpha}_{2\to 0} = \int_{-\infty}^{+\infty} u_2^*(x,\alpha)\, u_0(x)\,\mathrm{d}x \tag{109}$$

$$= \frac{1}{\sqrt{2}}\int u_0^*(x)u_0(x)\Big\{-1+\mathrm{j}\frac{2\pi\alpha}{\lambda}x-\frac{\alpha^2}{x_0^2}x^2+4\frac{1-\alpha^2}{x_0^2}x^2+\frac{2\pi^2\alpha^2}{\lambda^2}x^2 \tag{110}$$

$$-\mathrm{j}\frac{8\pi\alpha}{\lambda}x^3+\frac{4\alpha^2}{x_0^4}x^4-\frac{8\pi^2\alpha^2}{\lambda^2x_0^2}x^4+\mathcal{O}(\alpha^3)\Big\}\mathrm{d}x \tag{111}$$

$$= \frac{1}{\sqrt{2}}\Big\{-1+\big(\frac{4-4\alpha^2-\alpha^2}{x_0^2}+\frac{2\pi^2\alpha^2}{\lambda^2}\big)\frac{x_0^2}{4}+\big(\frac{4\alpha^2}{x_0^4}-\frac{8\pi^2\alpha^2}{\lambda^2x_0^2}\big)\frac{3}{16}x_0^4+\mathcal{O}(\alpha^3)\Big\} \tag{112}$$

$$= -\frac{\alpha^2}{\sqrt{2}}\big(\frac{1}{\theta_D^2}+\frac{1}{2}\big) \qquad \text{with } \theta_D=\frac{\lambda}{\pi x_0} \tag{113}$$

D TEM00 losses: other calculation method

D.1 TEM00 losses due to a translation of mode TEM00

In this appendix, we derive the translated fundamental mode function as a sum of the first order modes of the OMC.

The beam amplitude function is described along its propagation direction z as:

$$\phi(x) = A(t)\times u_0(x)\times u_0(y) = \mathcal{A}(t,y)\times u_0(x) \tag{114}$$

Inserting the full expression of u_0 in this equation and developping the exponential, the

shifted beam can be calculated by:

$$\begin{aligned}
\phi(x,,y,t,a) &= \mathcal{A}(t,y)\times\left(\frac{\sqrt{2}}{\sqrt{\pi}x_0}\right)^{1/2} e^{-\frac{(x-a)^2}{x_0^2}} && (115)\\
&= \mathcal{A}(t,y)\times\left(\frac{\sqrt{2}}{\sqrt{\pi}x_0}\right)^{1/2} e^{-\frac{x^2}{x_0^2}}\, e^{\frac{2ax}{x_0^2}}\, e^{-\frac{a^2}{x_0^2}} && (116)\\
&\sim \mathcal{A}(t,y)\,u_0(x)\times\left(1+\frac{2ax}{x_0^2}+\frac{2a^2x^2}{x_0^4}+\mathcal{O}(a^3)\right)\left(1-\frac{a^2}{x_0^2}+\mathcal{O}(a^4)\right) && (117)\\
&\sim \mathcal{A}(t,y)\left(1-\frac{a^2}{x_0^2}\right)\left[u_0(x)\left(1+\frac{a^2}{2x_0^2}\right)+u_1(x)\left(\frac{a}{x_0}\right)+u_2(x)\left(\frac{a^2}{\sqrt{2}x_0^2}\right)+\mathcal{O}(a^3)\right] && (118)\\
&\sim \mathcal{A}(t,y)\left[u_0(x)\left(1-\frac{a^2}{2x_0^2}\right)+u_1(x)\left(\frac{a}{x_0}\right)+u_2(x)\left(\frac{a^2}{\sqrt{2}x_0^2}\right)+\mathcal{O}(a^3)\right] && (119)\\
& && (120)
\end{aligned}$$

Defining $X=\frac{a}{x_0}$ gives:

$$\phi(x,y,t,a) \sim A(t)u_0(y)\left[\left(1-\frac{1}{2}X^2\right)u_0(x)+Xu_1(x)-\frac{1}{\sqrt{2}}X^2u_2(x)+\mathcal{O}(a^3)\right] \quad (121)$$

The component along the fundamental mode is found as in section 3.1.1.

D.2 TEM00 losses due to a tilt of the TEM00 mode

D.2.1 Effect of a beam tilt: only a delay

Let's assume that the beam is detected by a detector sensitive to the Hermite-Gaussian modes (TEM), but that the beam axis is tilted by the angle α related to the detector optical axis. The detector will then see the beam as a superposition of different modes.

The beam waist is supposed to be correctly adapted to the detector waist. The calculation is done going up to the 2nd order in α. The y-axis is choosen as the rotation axis of the beam: the component of the field along y is not modified.

The beam amplitude function is described along its propagation direction z as:

$$\phi(x,y,t) = A(t)\times u_0(x)\times u_0(y) = \mathcal{A}(y,t)\times u_0(x) \quad (122)$$

Along the detector optical axis, the tilt is seen as a modification of the path depending on the x position: $\delta z = x\sin(\alpha) = x\alpha+\mathcal{O}(\alpha^3)$. It is seen as a phase shift of $\frac{2\pi x\alpha}{\lambda}$ where λ is the laser wavelength.

Inserting the full expression of u_0 in this equation and developping the exponential, the

shifted beam can be calculated by:

$$\begin{aligned}\phi(x,y,t,\alpha) &= \mathcal{A}(y,t)\times u_0(x)e^{\mathrm{j}\frac{2\pi x\alpha+\mathcal{O}(\alpha^3)}{\lambda}} &(123)\\ &= \mathcal{A}(y,t)\times u_0(x)\left(1+\mathrm{j}\frac{2\pi x\alpha}{\lambda}-\frac{2\pi^2x^2\alpha^2}{\lambda^2}+\mathcal{O}(\alpha^3)\right) &(124)\\ &= \mathcal{A}(y,t)\left[u_0(x)\big(1-\frac{\pi^2\alpha^2x_0^2}{2\lambda^2}\big)+u_1(x)\big(\mathrm{j}\frac{\pi\alpha x_0}{\lambda}\big)-u_2(x)\big(\frac{\pi^2\alpha^2x_0^2}{\sqrt{2}\lambda^2}\big)+\mathcal{O}(\alpha^3)\right] &(125)\end{aligned}$$

Defining $\theta_D=\frac{\lambda}{\pi x_0}$ (the far-field diffraction angle of the fundamental mode) gives:

$$\phi(x,y,t,\alpha) = A(t)u_0(y)\left[\big(1-\frac{1}{2}\frac{\alpha^2}{\theta_D^2}\big)u_0(x)+\mathrm{j}\frac{\alpha}{\theta_D}u_1(x)-\frac{1}{\sqrt{2}}\frac{\alpha^2}{\theta_D^2}u_2(x)+\mathcal{O}(\alpha^3)\right] \quad (126)$$

Defining $X=\frac{\pi\alpha x_0}{\lambda}=\frac{\alpha}{\theta_D}$ gives:

$$\phi(x,y,t\alpha) = \mathcal{A}(y,t)\left[\big(1-\frac{1}{2}X^2\big)u_0(x)+\mathrm{j}Xu_1(x)-\frac{1}{\sqrt{2}}X^2u_2(x)+\mathcal{O}(\alpha^3)\right] \quad (127)$$

D.2.2 Effect of a beam tilt

The beam amplitude function is described along its propagation direction z as:

$$\phi(x) = \mathcal{A}(y,t)\times u_0(x) \quad (128)$$

The more complete description of the tilted field is given in section 3.1.2. The full expression of the tilted $u_0(x,\alpha)$ is given in equation 16. Developping the exponentials, the expresion of the tilted beam, projected along onto the OMC mode basis is:

$$\begin{aligned}\phi(x,y,\alpha) &= \mathcal{A}(y,t)\times u_0(x)e^{\frac{x^2\alpha^2}{x_0^2}}e^{-\frac{x^2\alpha^4}{4x_0^2}}e^{\mathrm{j}\frac{2\pi x\alpha+\mathcal{O}(\alpha^3)}{\lambda}} &(129)\\ &= \mathcal{A}(y,t)\times u_0(x)\left(1+\frac{x^2\alpha^2}{x_0^2}+\mathcal{O}(\alpha^4)\right)\left(1+\mathcal{O}(\alpha^4)\right)\left(1+\mathrm{j}\frac{2\pi x\alpha}{\lambda}-\frac{2\pi^2x^2\alpha^2}{\lambda^2}+\mathcal{O}(\alpha^3)\right) &(130)\\ &= \mathcal{A}(y,t)\left[u_0(x)\big(1-\alpha^2\big(\frac{\pi^2x_0^2}{2\lambda^2}+\frac{1}{4}\big)\big)+u_1(x)\big(\mathrm{j}\frac{\pi\alpha x_0}{\lambda}\big)\right. &(131)\\ &\qquad \left.-u_2(x)\frac{\alpha^2}{\sqrt{2}}\big(\frac{\pi^2x_0^2}{\lambda^2}-\frac{1}{2}\big)+\mathcal{O}(\alpha^3)\right] &(132)\end{aligned}$$

With $\theta_D=\frac{\lambda}{\pi x_0}$ and $\frac{1}{\theta_D}\gg 1$:

$$\phi(x,y,\alpha) \sim \mathcal{A}(y,t)\left[u_0(x)\big(1-\frac{\alpha^2}{2\theta_D^2}\big)+u_1(x)\,\mathrm{j}\,\frac{\alpha}{\theta_D}-u_2(x)\big(\frac{\alpha^2}{\sqrt{2}\theta_D^2}\big)+\mathcal{O}(\alpha^3)\right] \quad (133)$$

The result is the same as in equation 127 when only the tilt-induced delay is taken into account. The component along the fundamental mode is the same as found in equation 19.